

## THE "LEADING"-PARTICLE EFFECT IN INELASTIC N-N AND $\pi$ -N COLLISIONS

BY V. S. BARASHENKOV AND N. V. SLAVIN

Joint Institute for Nuclear Research, Dubna\*

(Received August 3, 1982)

Characteristics of the high-energy component of particles produced in inelastic hadron-hadron collisions at energies of  $5\text{--}5 \times 10^3$  GeV are analysed on the basis of the phenomenological approximation of known experimental data and Monte-Carlo modelling of individual acts of collision. Qualitative distinctions from the average characteristics of the particles produced become apparent at kinetic energies  $\tau \geq 0.2 \tau_{\text{MAX}}$ , where  $\tau_{\text{MAX}} = \sqrt{s}/2 - M$  is the highest possible energy of these particles. A number of methods for separating the "leading" particles are considered. Most of these particles are nucleons, even in the case of  $\pi$ -N collisions. The "leading" particles are produced mainly at the periphery of the interaction region. At  $\tau > 0.5 \tau_{\text{MAX}}$  the "leading" particle is the fastest one in every act of interaction.

PACS numbers: 13.85.-t, 13.85.Hd

As is generally known, in the inelastic interactions of high energy hadrons most of the colliding particles energy is usually carried off by several (one in the laboratory system) "leading" particles with sharply peaked energy. A great number of papers (see, e.g., Refs [1-6] for a further bibliography) has been devoted to the investigation of the properties of these particles and the conditions under which they can be formed. Unfortunately, the known experimental data are rather incomplete and sparse and much of them are obtained by analysis of hadron-nucleus collisions with a very rough consideration of intranuclear interactions. In addition, various authors use different criteria in defining the "leading" particle. As a result, one can presently have a rather approximate notion of the properties and the peculiarities of the high energy component of the secondary particles. However, the information already available points to the specific mechanism of this component production. An investigation of this mechanism could prompt the ways to construct a theory for hadron interactions at high and super high energies.

In our paper [7] the phenomenological approximation for inclusive spectra of sec-

---

\* Address: Joint Institute for Nuclear Research, Head Post Office, P.O. Box 79, 101000 Moscow, USSR.

ondary particles  $Ed^3\sigma/d^3p$  has been obtained which describes well the experimental energy and angular distributions of the particles produced, and the observed multiplicity of these particles in the wide range of energies from 5 GeV to several thousands of GeV. This approximation accumulates a great body of experimental data concerning particle spectra at both low and high kinetic energies  $\tau^1$ , and can be used for a systematic study of the properties of the high energy component of different types of secondaries and for the comparison of different ways of the quantitative description of the "leading"-particle effect. Consideration of these issues is the aim of the present paper.

TABLE I

The average number of high-energy particles  $\langle n \rangle = \langle n_N \rangle + \langle n_\pi \rangle$  in p-p and  $\pi^-$ -p interactions at energy  $T$

	$T, \text{ GeV} \backslash \tau/\tau_{\text{MAX}}$	0.2	0.4	0.7
p-p	10	1.7	1.0	0.48
	$10^2$	1.9	1.0	0.48
	$10^3$	1.9	1.0	0.48
$\pi^-$ -p	10	2.0	1.1	0.47
	$10^2$	2.3	1.1	0.51
	$10^3$	2.6	1.2	0.51

Table I and Figs. 1, 2 show how many particles with kinetic energy higher than  $\tau$  are produced in inelastic p-p and  $\pi^-$ -p collisions:

$$\langle n(\tau, s) \rangle = \{ \sigma_+[1, \tau, s] + \sigma_-[1, \tau, s] \} / \sigma_{\text{in}}, \quad (1)$$

where the functionals

$$\sigma_+[z, \tau, s] = \frac{\pi\sqrt{s}}{2} \int_{x(\tau)}^{x(\tau_{\text{MAX}})} \varphi_+[z, x, s] dx, \quad \sigma_-[z, \tau, s] = \frac{\pi\sqrt{s}}{2} \int_{-x(\tau_{\text{MAX}})}^{-x(\tau)} \varphi_-[z, x, s] dx$$

$$\varphi_{\pm}[z, x, s] = \int_0^{p_{\perp}(x, \tau)} \left( E \frac{d^3\sigma(x, p_{\perp}^2, s)}{d^3p} \right)_{\pm} \frac{z(\pm|x|, p_{\perp}^2, s) dp_{\perp}^2}{(x^2s/4 + p_{\perp}^2 + M^2)^{1/2}},$$

$$p = \sqrt{\tau(\tau + 2M)}, \quad x(\tau) = 2p/\sqrt{s}, \quad p_{\perp}^2(x, \tau) = p^2 - x^2s/4,$$

<sup>1</sup> Below we always use the centre-of-mass system and the following notation:  $\sqrt{s}$  is the total energy of the colliding particles,  $E = \tau + M$  and  $\tau$  are respectively the total and kinetic energies of the secondary particle considered,  $p_{\parallel}$  and  $p_{\perp}$  are the longitudinal and transversal momenta of this particle,  $x = 2p_{\parallel}s^{-1/2}$ .  $T$  is the kinetic energy of the projectile in the laboratory system. In the case of  $\pi$ -N interactions the region of  $x > 0$  (where the particle emission angles  $\theta < \pi/2$ ) corresponds to the direction of the primary meson motion.

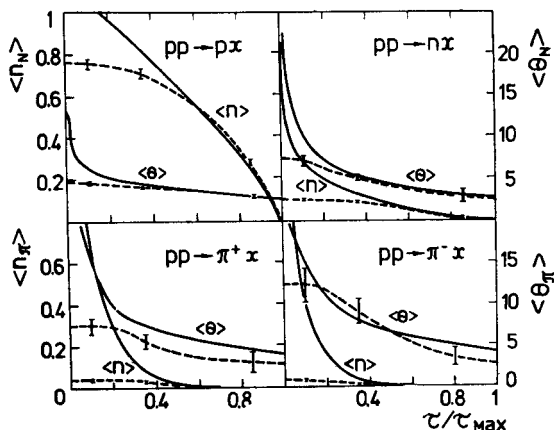


Fig. 1. The average number of secondary particles,  $\langle n \rangle$ , with kinetic energies higher than  $\tau$ , and  $\langle \theta \rangle$ , and the average emission angle of these particle in the inelastic p-p interaction at  $T = 100 \text{ GeV}$ . The dashed curves represent the corresponding distributions for the fastest secondary particle, calculated by the Monte-Carlo method. The statistical errors are shown

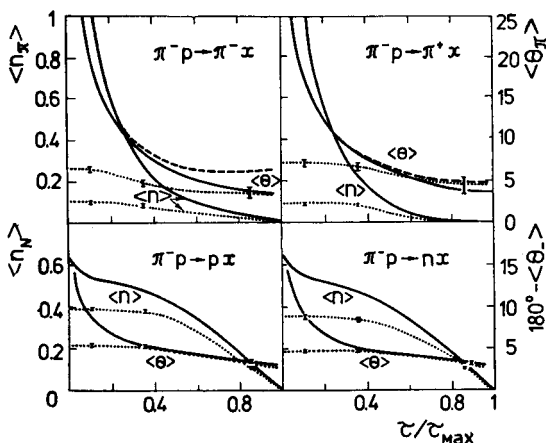


Fig. 2. Same as in Fig. 1, for the inelastic  $\pi^-p$  interaction at  $T = 100 \text{ GeV}$ . The values of  $\langle \theta_+ \rangle$  and  $\langle \theta_- \rangle$  are plotted by solid and dashed curves, respectively, the dotted curves represent the average multiplicity and average emission angle  $\langle \theta_+ \rangle = \langle \theta_- \rangle$  of the fastest secondary particle, calculated by the Monte-Carlo method. The statistical errors are given for these curves

$\tau_{\text{MAX}} = (s + M^2 - M_x^2)/(2\sqrt{s}) - M$ ,  $M_x$  is the minimum mass of the nascent particles after deducting the mass of the particle considered<sup>2</sup>,  $\sigma_{\text{in}}$  is the experimental total inelastic interaction cross-section. The indices “+” and “-” correspond to fore- and back hemispheres with respect to the direction of the projectile motion. It should be noted that the spectra  $Ed^3\sigma/d^3p$  for  $x > 0$  and  $x < 0$  are described by different formulae [7]. In Figs. 1, 2 the

<sup>2</sup> In reactions  $a+b \rightarrow c+X$ , if  $(a \equiv c, b \equiv c)$ ,  $(a \neq c)$ ,  $(a = N, c = \pi)$ , mass  $M_x$  is equal, respectively, to  $M_N, M_N + M_\pi, 2M_N$ , where  $M_N$  is the nucleon mass and  $M_\pi$  is the pion mass.

primary energy  $T = 100$  GeV is considered as an example, the picture being similar at other energies.

From Table I it follows that the number of high energy particles does not depend on the projectile energy  $T$  and varies rather slowly from one reaction to another. Figs. 1 and 2 demonstrate that the particles distinguished in energy are mostly those which have the same electric charge and baryon number as the colliding particles have. The production of high energy particles with charge signs differing from that of the primary one is less probable. In the case of N-N collisions the probability of the "leading"-meson emission is very small. In  $\pi$ -N collisions where the primary meson and nucleon are in similar kinematic conditions, the nucleon, however, turns out to be distinguished by its energy at  $\tau > 0.3 \tau_{\text{MAX}}$  more often than the meson (see Table II). Figs. 1, 2 and Table III, IV represent the average values of the angle of particle emission into the fore- and back- hemispheres

$$\langle \theta_{\pm}(\tau, s) \rangle = \sigma_{\pm} \left[ \arctg \left( \frac{p_{\perp}}{p_{\parallel}} \right), \tau, s \right] / \sigma_{\pm}[1, \tau, s]. \quad (3)$$

TABLE II

The ratio of the average numbers of high-energy nucleons and mesons  $\langle n_N \rangle / \langle n_{\pi} \rangle$  in p-p and  $\pi^-$ -p collisions at energy  $T$

	$T, \text{ GeV}$	$\tau/\tau_{\text{MAX}} > 0.2$	$\tau/\tau_{\text{MAX}} > 0.4$	$\tau/\tau_{\text{MAX}} > 0.7$
p-p	10	2.3	8	$\sim 100$
	$10^2$	1.6	8	$\sim 100$
	$10^3$	1.5	8	$\sim 100$
$\pi^-$ -p	10	0.61	1.6	4.2
	$10^2$	0.52	1.5	4.2
	$10^3$	0.43	1.4	4.2

TABLE III

The average emission angle (in degrees) for high-energy protons  $\langle \theta_p \rangle$  in p-p and  $\pi^-$ -p collisions at energy  $T$

	$T, \text{ GeV}$	$\tau/\tau_{\text{MAX}} > 0.2$	$\tau/\tau_{\text{MAX}} > 0.4$	$\tau/\tau_{\text{MAX}} > 0.7$
p-p	10	15	11	10
	$10^2$	5.1	4.0	3.2
	$10^3$	2.0	1.5	1.1
$\pi^-$ -p	10	16	14	11
	$10^2$	7	5.2	3.8
	$10^3$	4	1.7	1.3

TABLE IV

The ratio of the multiplicities of the high-energy mesons emitted into the fore- and backward hemispheres in  $\pi^-$ -p interactions,  $\sigma_+[1, \tau, s]/\sigma_-[1, \tau, s]$

$T, \text{ GeV}$	$\tau/\tau_{\text{MAX}} > 0.2$	$\tau/\tau_{\text{MAX}} > 0.4$	$\tau/\tau_{\text{MAX}} > 0.7$
10	1.6	2.2	5.8
$10^2$	1.6	2.1	6.8
$10^3$	1.6	2.1	9.3

In p-p collisions the angle  $\langle\theta_+\rangle = \langle\theta_-\rangle$ ; in  $\pi^-$ -p collisions the nucleons are practically absent in the forward hemisphere, that is why the nucleon angle  $\langle\theta_+\rangle$  is not indicated.

The high energy nucleons are produced mainly in a narrow space angle around the primary proton velocity vector. Mesons with high kinetic energy are also emitted into a narrow angle around the direction of the primary particle motion. In the  $\pi^-$ -p reaction such mesons are produced, as a rule, in the hemisphere corresponding to the direction of the projectile pion velocity and only few particles fly out into the opposite hemisphere (see Table IV)<sup>3</sup>. Figs. 1 and 2 show that usually the mesons fly out into a wider angle than the nucleons. The emission angles of the high energy particles  $\langle\theta\rangle$  depend weakly on the type of reaction and decrease with increasing primary energy  $T$ .

In Fig. 3, the distributions of the radius of the space region connected with the production of high energy particles are exemplified for p-p and  $\pi^-$ -p collisions at  $T = 100 \text{ GeV}$ .

$$\langle\varrho(\tau, s)\rangle = \hbar/\langle p_{\perp}(\tau, s)\rangle = \hbar\sigma_{\text{in}}\langle n(\tau, s)\rangle/\{\sigma_+[p_{\perp}, \tau, s] + \sigma_-[p_{\perp}, \tau, s]\}. \quad (4)$$

The particle emission occurs mainly in the region of  $\varrho \sim (0.4-0.7) \times 10^{-13} \text{ cm}$ . In this case nucleons are produced at greater, on the average, values of  $\varrho$ . The mean  $\langle\varrho\rangle$  is slightly sensitive to the energy  $T$  of the primary particle (see Table V).

The characteristic features of the "leading" effect can be understood by assuming that the high energy nucleons are generated mainly in grazing peripheral collisions in which only a small part of the total energy  $\sqrt{s}$  turns into the meson component, this part decreasing as the interaction becomes more peripheral. It is essential that the mechanism of the grazing collisions remains predominant in a wide range of energies up to  $T \sim 10^3 \text{ GeV}$  at which spectrum measurements for the produced particles are still accessible. This conclusion is confirmed by the whole totality of the presently available experimental data.

<sup>3</sup> The emission of few mesons leads to a significant increase in the average meson emission angle near  $\theta \sim \pi$

$$\langle\theta\rangle = \{\langle\theta_+\rangle\sigma_+ + \langle\theta_-\rangle\sigma_-\}/\{\sigma_+ + \sigma_-\}.$$

For example, at  $T = 100 \text{ GeV}$  the angle  $\langle\theta_-\rangle$  exceeds  $\langle\theta_+\rangle$  by almost one order of magnitude for the "leading" mesons with energies  $\tau > 0.7 \tau_{\text{MAX}}$ . Therefore a separate consideration of the angles  $\langle\theta_+\rangle$  and  $\langle\theta_-\rangle$  is more illustrative.

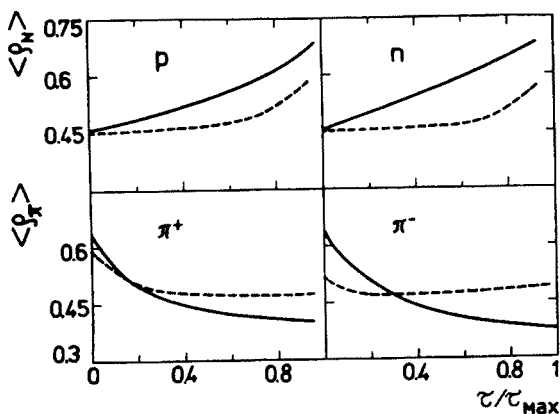


Fig. 3. The distribution of the average distances at which the particles with kinetic energies higher than  $\tau$  are produced. The solid and dashed curves correspond to the inelastic p-p and  $\pi^-$ -p interactions, respectively. The initial energy is  $T = 100$  GeV

From the data given above it is seen that there is no strict distinction between the "leading" particles and other secondaries. The frequently used separation criterion  $\tau_{\text{lab.}} > 0.7 T$ , i.e.  $\tau > (0.3-0.4) \sqrt{s} \approx (0.6-0.8)\tau_{\text{MAX}}$  is rather conventional. Although the "leading" particle effect becomes more pronounced as the ratio  $\tau/\tau_{\text{MAX}}$  increases, one can consider as leading particles those with  $\tau > 0.2\tau_{\text{MAX}}$  at  $T = 100$  GeV and with  $\tau > 0.1\tau_{\text{MAX}}$

TABLE V

The average radius of the space region,  $\langle \rho \rangle 10^{-13}$  cm, where the production of nucleons and pions with energies  $\tau > 0.7 \tau_{\text{max}}$  occurs

	$T, \text{ GeV}$	$\langle \rho_N \rangle$	$\langle \rho_\pi \rangle$
p-p	10	0.65	0.51
	$10^2$	0.58	0.43
	$10^3$	0.55	0.41
$\pi^-$ -p	10	0.52	0.53
	$10^2$	0.49	0.47
	$10^3$	0.48	0.44

at  $T = 10^3$  GeV. For the overwhelming majority of these particles the condition  $\theta \sim 0$  or  $\theta \sim \pi$ , used by some authors as an additional criterion for selection of leading particles, is satisfied.

The authors of paper [4] suggest to regard as a "leading" particle that secondary particle which has the highest kinetic energy in the given act of inelastic interaction, irrespective of whether or not this energy satisfies the criterion  $\tau > a\tau_{\text{MAX}}$  with some fixed coefficient  $a$ . (At high energies such a particle is, at the same time, the fastest one although the velocities of most of the secondaries are close to light velocity and it is rather difficult

to discriminate between them). In theory one can simulate the proposed separation of the "leading" particle by the Monte-Carlo method, which allows one to calculate the multiplicity, emission angles and energies for all the secondaries for each inelastic interaction with the help of then known cross-section  $Ed^3\sigma/d^3p$  and the energy-momentum conservation law<sup>4</sup>.

In the centre-of-mass system where, according to the momentum conservation law, the production of the particle with high energy and small emission angle  $\theta \sim 0$  is usually accompanied by the formation of the compensating very fast particle in the region of  $\theta \sim \pi$ , the identification of the leading particle as the most energetic (fastest) one selects only a part of all high energy particles:  $\Delta_i(\tau) \equiv n_i(\tau) - n_i(\tau)_{\text{MAX } \tau}$ , ( $i = p, n, \pi$ ). The sum of the multiplicity differences

$$\int_0^{\tau_{\text{MAX}}} \{\Delta_p(\tau) + \Delta_n(\tau) + \Delta_\pi(\tau)\} d\tau = \langle n \rangle - 1$$

can be rather significant. However, at  $\tau > 0.5\tau_{\text{MAX}}$  the difference is small and entirely determined by the contribution of  $\pi$ -mesons; for nucleons  $n(\tau) \simeq n(\tau)_{\text{MAX } \tau}$  (see Figs 1, 2 and Table VI).

TABLE VI

The probabilities (%%) for the proton, neutron or pion to be the fastest secondary particle. The initial energy  $T = 100$  GeV

Particle \ Collision	P-P	$\pi$ -P
p	75 ± 2.5	39 ± 1.5
n	11 ± 1	34 ± 1.5
$\pi^-$	3 ± 0.5	11 ± 0.5
all $\pi$	14 ± 1	27 ± 1
$(p+n)/\pi$	6.1 ± 0.6	2.7 ± 0.1

As a rule (even in the case of  $\pi$ -N collisions) it is a nucleon that appears to be the most energetic particle. The probability of the meson to be distinguished by its energy is considerably smaller, being negligibly small in the region of  $\tau > 0.5\tau_{\text{MAX}}$ .

<sup>4</sup> Some approach to the Monte-Carlo simulation of inelastic collisions is described in papers [8] and, in more detail, in the monograph [9]. A similar method is used in the present case. An essential distinction lies in the replacement of a polynomial approximation of cross-sections by a more complicated one based on the phenomenological expressions from [7] and in the application of majorizing expressions to speed up the tossing of the  $x$  and  $p_\perp$  values. For each particle "c" produced, the sampling of these quantities was preceded by the electric charge sign sampling on the basis of the relative probabilities

$$\sigma(s, a+b \rightarrow c+\dots) / \sum_k \sigma(s, a+b \rightarrow c_k+\dots) = \langle n_c(s) \rangle / \sum_k \langle n_{c_k}(s) \rangle.$$

The total multiplicity of the particles produced was fixed by the law of energy and momentum conservation, as in Refs. [8, 9].

As the average multiplicity, the angular distributions of all high-energy nucleons with  $\tau > 0.5 \tau_{\text{MAX}}$  and the "fastest" ones practically coincide. These distributions are similar for the mesons as well. At the same time, in the N-N collision where the multiplicity of the "fastest" mesons is somewhat smaller than the total multiplicity of all high-energy mesons even at high  $\tau$  (Fig. 2), the emission angles of the latter are wider. This is explained by the contribution of the reaction channels involving the production of several high-energy particles at once.

As it can easily be seen, the selection of the "leading" particles in the absolute and relative values of  $\tau$  leads to the same result at high energies. The comparison of the two methods of selection at lower energies allows one to obtain an interesting additional information. Nevertheless, an experimental study of this problem requires a large amount of the events observed.

It should be emphasized that all the conclusions made above are not theoretical results, but the results of the phenomenological analysis of experimental data. Although the initial information is rather sparse (especially at high energies), the unification of the available data by means of a common approximation allows one to obtain the sufficiently complete picture of the inelastic collision of two hadrons.

A more precise description of the inelastic collision is associated with taking into account the resonance channels. As is well known, a considerable part of secondary particles is produced as a result of the decays of the resonances  $\omega$ ,  $\rho$  etc., while the above used expressions  $Ed^3\sigma/d^3p$  correspond to the final (at time  $t = \infty$ ) cross sections. The calculation of the decays can be performed very accurately and therefore the explicit separation of the resonance channel cross sections  $d^3\sigma_{\text{RES}}/d^3p$  enables one to improve the approximation of the cross-sections  $d^3\sigma/d^3p$  observed.

#### REFERENCES

- [1] A. Sh. Gaytinov et. al., *Yad. Fiz.* **24**, 350 (1976).
- [2] N. Angelov et al., Preprint JINR, 1-8064, Dubna 1974.
- [3] I. Ya. Chasnikov, *The "Leading"-Particle Effect in Hadron Interactions*, Doctor's Thesis, JINR 1-10696, Dubna 1977.
- [4] A. I. Anoshin et al., Preprint JINR, 1-10804, Dubna 1977.
- [5] L. A. Didenko, V. S. Murzin, L. I. Sarycheva, *The Asymmetry of Hadron Interaction*, Nauka, Moskva 1981.
- [6] M. Basile et al., *Lett. Nuovo Cimento* **32**, 321 (1981), Report CERN EP/81-86, Geneva 1981.
- [7] V. S. Barashenkov, N. V. Slavin, *Acta Phys. Pol.* **B12**, 563, 951, 959 (1981).
- [8] V. S. Barashenkov et al., *Acta Phys. Pol.* **36**, 457, 877 (1969).
- [9] V. S. Barashenkov, V. D. Toneev, *Interaction of High Energy Particles and Atomic Nucleus with Nucleus*, Atomizdat, Moskva 1972.